



Chemical evolution of dwarf spheroidal galaxies based on model calculations incorporating observed star formation histories

H. Homma and T. Murayama

Tohoku University Astronomical Institute, 6-3 Aramaki, Aoba-ku Sendai, Japan
e-mail: hide@astro.tohoku.ac.jp

Abstract. We investigate the chemical evolution model explaining the chemical composition and the star formation histories (SFHs) simultaneously for the dwarf spheroidal galaxies (dSphs). Recently, wide imaging photometry and multi-object spectroscopy give us a large number of data. Therefore, we start to develop the chemical evolution model based on an SFH given by photometric observations and estimates a metallicity distribution function (MDF) comparing with spectroscopic observations. With this new model we calculate the chemical evolution for 4 dSphs (Fornax, Sculptor, Leo II, Sextans), and then we found that the model of 0.1 Gyr for the delay time of type Ia SNe is too short to explain the observed $[\alpha/\text{Fe}]$ vs. $[\text{Fe}/\text{H}]$ diagrams.

Key words. Galaxies: abundances – Galaxies: dwarf – Galaxies: evolution – Local Group – Galaxies: stellar content

1. Introduction

Dwarf galaxies in the Local Group are good laboratories to study the galactic chemical evolution. In recent decades, the chemical evolution of the dwarf galaxies have been studied by both observational and theoretical approaches. By the observational approaches, the star formation histories (SFHs) of dwarf galaxies are derived from their color magnitude diagrams (CMDs). The chemical composition of their stars and gas are measured by spectroscopy.

In theoretical approaches, the chemical evolution is estimated by numerical calculations and/or hydrodynamical simulation. Kirby et al. (2010) observed a lot of stars in 8 dSphs by spectroscopy and measured their chemical abundances. And then Kirby et al. (2011) (hereafter K11) analyzed the data by their

chemical evolution model, but their derived SFHs were much shorter than that estimated from the CMDs. They concluded that the derived SFHs are extremely sensitive to the delay time for the first Type Ia supernova (SN Ia). To solve this problem, we use the observational SFHs directly in our model, and attempt to construct a chemical evolution model explaining both SFHs and MDFs of dSphs. Then we can evaluate the delay time for SN Ia within the chemical evolution time scale based on the observed SFHs.

2. The chemical evolution model

We construct the chemical evolution model to reproduce both of the observational SFHs and the observed MDFs at the same time. Our

model is basically the same as that of K11. The differences from K11 are described below;

1. Calculating the chemical evolution complying with the SFHs estimated from the photometric observations for each dSph.
2. The Delay Time Distribution function for SNe Ia is that observed by Maoz et al. (2010), same as K11. While K11 adopted 0.1 Gyr for the delay time for SNe Ia, we compare the models with the delay time of 0.1 Gyr and 0.5 Gyr.
3. The infall rate is not a pure functional form. Since we fix the SFH and adopt the Kennicutt-Schmidt law, the star formation rate (SFR) and the gas mass at each time is given. The gas mass ejected from the stars can be calculated from the assumed stellar yields, and the outflow rate is determined by the SFH as same as K11. Therefore, the infall rate is derived from the equations of chemical evolution at each time step.
4. We set the stellar lifetimes as those given by Timmes, et al. (1995). But this difference is not significant.

The equation of the chemical evolution for an element i is:

$$\dot{M}_{\text{gas},i}(t) = -\Psi(t)X_i(t) + E_i(t) + \dot{M}_{\text{in},i} - \dot{M}_{\text{out},i} \quad (1)$$

where $\dot{M}_{\text{gas},i}(t)$ is the time-derivative of the gas mass for i at any time, $\Psi(t)$ is the star formation rate, $X_i(t)$ is the mass fraction for i , and $E_i(t)$ is the gas mass for i ejecting to ISM. $\dot{M}_{\text{in},i}$ and $\dot{M}_{\text{out},i}$ are the infall and outflow gas mass respectively. We calculate the chemical evolution for many elements at each time steps ($\Delta t=25\text{Myr}$). The calculation is terminated when the star formation rate reaches zero.

Our chemical evolution model have three free parameters; A_* , A_{out} , and τ_{Ia} . A_* is the star formation efficiency, and A_{out} is the outflow gas mass when one SN event occurs, and τ_{Ia} is the delay time for SNe Ia.

3. Compare the model results with the observations

We calculate the chemical evolutions for four dSphs whose SFH and MDF were already ob-

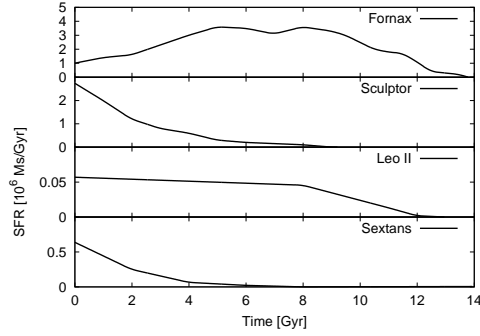


Fig. 1. The SFHs of dSphs derived from the CMDs. ((Fornax) de Boer et al. (2012a); (Sculptor) de Boer et al. (2012b); (Leo II) Dolphin (2002); (Sextans) Lee et al. (2009))

tained by the observations; Fornax, Sculptor, Leo II, and Sextans. Figure 1 shows the SFHs of our sample (Fornax: de Boer et al. 2012a, Sculptor: de Boer et al. 2012b, Leo II: Dolphin 2002, Sextans: Lee et al. 2009). We use the MDFs of Kirby et al. (2010) for all the sample dSphs. Note that the MDFs are convolved with Gaussian kernel with the observational errors.

We adopt χ^2 -method for comparing model results. The χ^2 is obtained for each parameter set (A_* , A_{out} , τ_{Ia}) from the equation (2)

$$\chi^2 = \left(\sum_{i=1}^{N_{\text{bin}}} \frac{(f_{i,\text{model}} - f_{i,\text{obs}})^2}{f_{i,\text{obs}}} \right) / \left(\sum_{i=1}^{N_{\text{bin}}} f_{i,\text{obs}} \right) \quad (2)$$

where $f_{i,\text{obs}}$ and $f_{i,\text{model}}$ are the stellar numbers, whose metallicities are i , for the observation and the model with one parameter set, respectively. N_{bin} is the total number of metallicity bins and we take it as $N_{\text{bin}} = 500$ from $[\text{Fe}/\text{H}] = -3.5$ to 1.0. To prevent the χ^2 diverge, we only calculate in the range $f_{i,\text{obs}} > 0.24$. This value corresponds 1σ of the probability distribution function for typical contribution of observed single star.

We compute the χ^2 in parameter space, and choose the optimum chemical evolution model which minimize the χ^2 for each dSph. The parameter ranges are; A_* [Gyr] = $[10^{-3}, 10]$, A_{out} [M_{\odot}/SN] = $[10^2, 10^5]$, τ_{Ia} [Gyr] = 0.1, 0.5. To see the effect of the delay time for the first SN Ia,

τ_{Ia} , we compute χ^2 for each parameter set and find the best fit model by χ^2 -minimum technique for the case of $\tau_{\text{Ia}}=0.1$ and 0.5, respectively.

4. Results and discussion

We show the results of our chemical evolution calculations in Figure 2. The best fit parameters are listed in Table 1. As shown in Figure 2 the MDFs are well reproduced by both models with $\tau_{\text{Ia}}=0.1$ Gyr and with 0.5 Gyr. On the other hand, the behaviors of models in [Mg/Fe] vs. [Fe/H] diagram are very different on τ_{Ia} . The model locus whose delay time is 0.5 Gyr well passes through the data points in this diagram, while the model with $\tau_{\text{Ia}}=0.1$ Gyr underestimate [Mg/Fe]. Therefore, our model prefer the models of $\tau_{\text{Ia}}=0.5$ Gyr.

In K11 their adopted $\tau_{\text{Ia}}=0.1$ Gyr from the observational result by Maoz et al. (2010). Nevertheless their models well predicted the diagrams of [Mg/Fe] vs. [Fe/H]. Since τ_{Ia} defines the time scale of chemical evolution, their derived SFH is much shorter than that estimated from the CMD observation. On the other hand, our model fixed the SFH as is observed, thus the given SFH determines the time scale of chemical evolution. Therefore, longer time scale of chemical evolution favors longer delay time for SNe Ia.

Consequently, to explain both of the SFH and the chemical abundances of dwarf galaxies at the same time, longer delay time for SNe Ia than observed by Maoz et al. (2010) is necessary. Recent observations and theoretical works show that the delay time for SNe Ia with shorter than 1 Gyr is natural, and its lower limit is about 0.1 Gyr (Totani et al. 2008, Maoz & Mannucci 2012). This discrepancy of delay time for SNe Ia may be caused by that the approximations in our model are too simple. In the model approximations, one-zone assumption, instantaneous mixing approximation (IMA), and initial mass function (IMF) are discussed in many previous works.

The one-zone is a very simple picture for studying about the chemical evolution of galaxies, because the galaxies have some components like as bulge, halo, disk, and some galax-

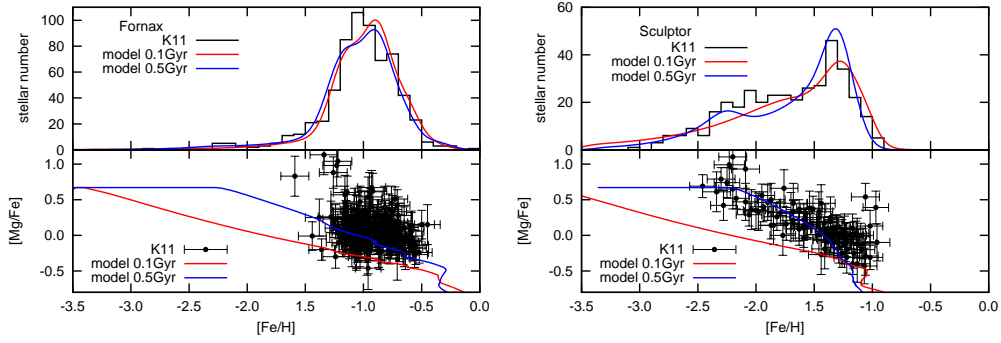
ies experience a merger event. Even dwarf galaxies, there are age and metallicity gradients in Fornax and Sculptor (de Boer et al. 2012a,b). Therefore, one-zone assumption in this model is conflict with the observed features. Moreover, the observed areas for SFHs and MDFs adopted in our models are different. The photometric areas for SFHs are much larger than the spectroscopic areas for MDFs. The IMA is a very critical approximation affecting the delay time of SNe Ia. Since we assumed IMA, SNe ejecta is well mixed with the interstellar matter and contributes to the star formation within shorter time than the calculation time step (25 Myr in our model). This is apparently oversimplified assumption, and we must consider the typical duration of gas recycling after the SNe explosion. The longer delay time, which our model favors, may include not only the delay of SNe Ia but also time scale of the gas recycling.

The IMF also plays critical role in the chemical evolution and is more complicated. In our model, we set the stellar mass range from $0.08 M_{\odot}$ to $100 M_{\odot}$, same as K11. Generally, the chemical evolution model assume that the IMF has no time evolution. However in the zero or extremely low metal galaxies, the gas cooling may be more inefficient than metal-rich environment and then a large number of massive stars may be formed. Resulting top-heavy IMF will change the speed of chemical enrichment and the stellar age distribution, and then the discrepancy of the results may be relaxed.

To investigate the chemical evolution of dwarf galaxies, chemical composition of metal poor stars is critical. For example, [Mg/Fe] does not change in the earliest epochs before the first SN Ia appears, and a plateau region at lower [Fe/H] is expected in the diagram of [Mg/Fe] vs. [Fe/H]. When SNe Ia start to explode, [Mg/Fe] rapidly decreases with [Fe/H] increases, thus the [Fe/H] of the breaking point of [Mg/Fe] corresponds the metallicity when the first SN Ia appeared. Confirming this behavior observationally is expected to provide a good limit of the delay time in our model. However, while Kirby et al. (2010) provided chemical abundance data for the largest

Table 1. The parameter sets of each optimum model

| dSph | $\tau_{\text{Ia}} = 0.1\text{Gyr}$ | | | $\tau_{\text{Ia}} = 0.5\text{Gyr}$ | | |
|----------|------------------------------------|--|----------------------|------------------------------------|--|----------------------|
| | A_* [$10^{-2}/\text{Gyr}$] | A_{out} [$10^3 M_{\odot}/\text{SN}$] | reduced- χ^2 | A_* [$10^{-2}/\text{Gyr}$] | A_{out} [$10^3 M_{\odot}/\text{SN}$] | reduced- χ^2 |
| Fornax | 3.2 | 1.6 | 0.70 | 7.9 | 1.3 | 0.62 |
| Sculptor | 1.3 | 6.3 | 2.0 | 10 | 5.0 | 1.65 |
| Leo II | 0.4 | 4.0 | 0.39 | 1.6 | 5.0 | 1.28 |
| Sextans | 0.8 | 16 | 0.58 | 13 | 10 | 0.83 |

**Fig. 2.** The MDFs (upper panels) and $[\text{Mg}/\text{Fe}]$ vs. $[\text{Fe}/\text{H}]$ (lower panels) of Fornax and Sculptor. Black lines and black dots with error bars are the observational results by Kirby et al. (2010). Note that we show the observational MDFs as histograms of stars whose $[\text{Fe}/\text{H}]$ uncertainties are less than 0.3 dex. Blue lines are the models with $\tau_{\text{Ia}}=0.1\text{Gyr}$ and red lines are those with $\tau_{\text{Ia}}=0.5\text{Gyr}$.

and homogeneous sample, the plateau region and the breaking point in $[\text{Mg}/\text{Fe}]$ vs. $[\text{Fe}/\text{H}]$ are still unclear. Moreover, the dispersion of $[\text{Mg}/\text{Fe}]$ at the plateau region may give a hint for chemical homogeneity in the system. We also expect that the mass range of IMF, especially its lower limit, in the extremely metal poor environment can be investigated by obtaining $[\text{Mg}/\text{Fe}]$ of the metal poor stars.

References

de Boer, T. J. L., et al. 2012b, *A&A*, 539, 103

- de Boer, T. J. L., et al. 2012a, *A&A*, 544, 73
 Dolphin, A. E. 2002, *MNRAS*, 332, 91
 Kirby, E. N., et al. 2010, *ApJS*, 191, 352
 Kirby, E. N., et al. 2011, *ApJ*, 727, 78 (K11)
 Lee, M. G., et al. 2009, *ApJ*, 703, 692
 Maoz, D., Sharon, K., & Gal-Yam, A. 2010, *ApJ*, 722, 1879
 Maoz, D., & Mannucci, F. 2012, *PASA*, 29, 447
 Totani, T., et al. 2008, *PASJ*, 60, 1327